RESULTS OF CALIBRATION FOR GOSAT TANSO

Tomoko Kina [a], Kei Shiomi [a], Shuji Kawakami [a], *
Yasushi Mitomi [b], Mayumi Yoshida [b], Riko Higuchi [b], Nami Sekio [b], Fumie Kataoka [b]

[a] Japan Aerospace Exploration Agency, 2-1-1 Sengen, Tsukuba, Ibaraki 305-8505, Japan - kawakami.shuji@jaxa.jp
[b] Remote Sensing Technology Center of Japan, 1-6-1 Takezono, Tsukuba, Ibaraki 205-0032, Japan

Commission VIII, JAXA Special Session

KEY WORDS: GOSAT, greenhouse gases, FTS

ABSTRACT:

GOSAT (Greenhouse gases Observing SATellite) was launched on January 23, 2009. After the initial functional check-out, which was completed in early April 2009, initial calibration was conducted over the following 3 months. Calibration accuracy of the TANSO-FTS was evaluated on radiance, spectral characteristics, and geometry. Radiometric accuracy was evaluated using two methods: onboard calibration and vicarious calibration. Onboard calibration was performed using calibration data. To evaluate the radiometric sensitivity of the sensors, solar irradiances were used for SWIR bands with the Kurucz solar irradiance model. For the TIR band, deep space and blackbody data were used. Vicarious calibration was done to compare the observed radiance of GOSAT with the radiance calculated by Pstar (Ota et al., 2009). As a result of the two methods, the radiometric accuracy of the TANSO-FTS (SWIR) is estimated at 10 percent. The calibrated Level 1B products were released on October 30, 2009. Calibration factors were partly modified and the information on the accuracy of radiometry and geometry was provided for data users.

1. INTRODUCTION

GOSAT observes global distributions of greenhouse gases (carbon dioxide: CO_2 and methane: CH_4) from space. Its operation time is 5 years from 2009 to 2013, which overlaps with the first commitment period of the Kyoto protocol. The mission objective is measuring global greenhouse gases with accuracies of 1 percent for CO_2 and 2 percent for CH_4 in seasonal mean. GOSAT observation data is used for global sub-continental scale flux estimation. GOSAT was launched on January 23, 2009. The Level 1 data has been released since September 2009; Level 2 data of CO_2 and CH_4 column-averaged volume mixing ratios since February 2010. GOSAT data from over 1 year has been acquired. The global distributions of CO_2 and CH_4 concentration were obtained in various seasons.

GOSAT is a joint project for the monitoring of greenhouse gases by the Ministry of the Environment (MOE), the National Institute for Environmental Studies (NIES), and the Japan Aerospace Exploration Agency (JAXA) (Yokota et al., 2004). The GOSAT satellite carries the Thermal And Near infrared Sensor for carbon Observation (TANSO) for precise measurement of greenhouse gases (Kuze et al., 2009).

The GOSAT sensors were characterized in a pre-flight test (PFT) (Yoshida et al., 2008). The Level 1 algorithm was developed using the evaluation of the PFT data. After the launch, the observation data was evaluated on orbit by onboard and vicarious calibration methods in the initial calibration and validation phase. The results were reflected in the improvement of the initial calibrated Level 1 algorithm. The initial calibrated Level 1 products are processed and delivered to the NIES by JAXA. The NIES provides the products to GOSAT research PIs.

2. INITIAL CALIBRATION AND VALIDATION PHASE

The initial calibration and validation phase was operated from April 11 to July 30 after the initial functional check-out phase. This phase aimed at obtaining intensive calibration and validation data and releasing initial calibrated Level 1 products after the calibration activities. The TANSO-FTS was pointed at calibration and validation sites in accordance with observation requests and in combination with multiple observation modes. The TANSO-CAI performed continuous swath observation.

2.1 TANSO-FTS Calibration and Validation Sites

The TANSO-FTS calibration and validation points are illustrated in Figure 1. The calibration and validation points acquired in the special observation mode are shown in red and green, respectively. The other calibration and validation points, shown in blue, were observed by normal observation and sun glint observation due to their proximity to existing observation points available for selection. Calibration points are ARM sites, Railroad valley, and the Sahara Desert. Validation points are composed of TCCON sites and JAL CONTRAIL airports. The TANSO-FTS observed these sites regularly in the initial calibration and validation phase and collected intensive observation data.

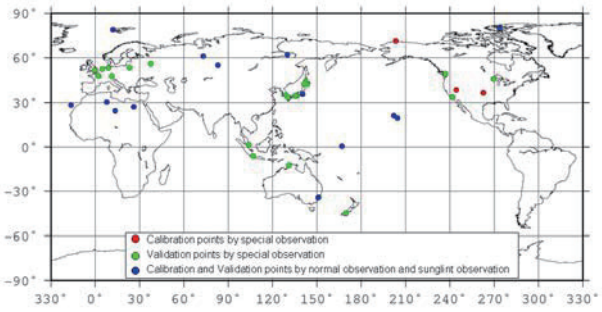

Figure 1. TANSO-FTS calibration and validation points.

3. INITIAL CALIBRATION RESULTS OF TANSO-FTS

3.1 Radiometric Calibration

3.1.1 Vicarious Calibration in the Sahara Desert

The Sahara Desert has high reflectance at SWIR bands. We investigated the Sahara Desert sites using MODIS data with high reflectance, homogeneity, and temporal stability to compare with other satellites and monitoring. We selected the nadir looking data of the TANSO-FTS to avoid the surface BRDF. The surface reflectance database was calculated from averaged MODIS Nadir BRDF-Adjusted Reflectance from 2005 to 2006. The Pstar2 was used in the line-by-line calculation of HITRAN 2004. The GPV provided by the JMA were used as atmospheric profiles. Relations between simulation and observation radiances of B1-3 are obtained. The radiances were compared in lower absorption wave numbers. The Kurucz solar irradiance model was used as solar reference database in the evaluation.

3.1.2 Summary of the Radiometric Calibration

The TANSO-FTS calibration factor is described as ratio of the referenced radiance relative to the Level 1B radiance after multiplying the radiometric conversion coefficient based upon the PFT calibration result. The recommended calibration factors by both methods are listed in Table 1. The results are similar, since the Kurucz solar irradiance model is commonly used for the referenced radiances. Initial calibration was restricted to the methods, sites, and data quantities; hence, the further calibration will be required.

TANSO-FTS Calibration Factor (= Referenced radiance[*1] / Level 1B radiance[*2])						
	B1P	B1S	B2P	B2S	B3P	B3S
Solar irradiance (gain M)	1.093	1.089	1.008	1.026	1.012	1.031
Sahara Desert [*3] (gain M)	1.129	1.121	1.031	1.030	1.010	1.003
Satellite coincidence [*3] (gain M)	1.103	1.098	1.053	1.050	1.044	1.034
Satellite coincidence [*3] (gain H)	1.068	1.041	1.059	1.046	1.102	1.079

Table 1. TANSO-FTS radiometric calibration factor of B1-3 for bias correction (average from April to July).
(*1) Referenced radiance originates from Kurucz Irradiance2005 for B1 and Irradiance2008 for B2 and B3. (*2) After multiplying the radiometric conversion coefficient. (*3) Comparison with radiative transfer calculation using MODIS surface reflectance, which is stable in temporal and spatial variations. Normally, the FTS is operated with gain H. At a high target, such as a desert, it is with gain M.

3.2 Geometric Calibration

The CMOS camera (CAM-H8) is installed on the TANSO-FTS to monitor the FTS IFOV at fine resolutions of 50-100 m. The CAM-H8 takes a visible image by clipping part of the incident light. Geometric accuracy is evaluated using ground control points (GCPs). ALOS AVNIR-2 images are used as a reference, which are well calibrated in geometry. We selected 17 images without clouds from April 18 to May 2 for initial calibration. Results of the geometric bias error pixels and geometric accuracy are listed in Table 2. Geometric accuracy is evaluated within the target accuracy of 1.3 km at sub-satellite. The geometric accuracy is under evaluation in the next period.

	Error in CAM-H8 Image (VGA-CUT)	Geometric Accuracy (RMSE)
Pixel (CT)	- 4.2 pixel	0.41 km
Line (AT)	+ 2.2 pixel	0.21 km

Table 2. TANSO-FTS geometric bias error until May 2.

4. INITIAL CALIBRATION RESULTS OF TANSO-CAI

4.1 Radiometric Calibration

4.1.1 Vicarious Calibration in the Sahara Desert

Radiometric calibration in the Sahara Desert was evaluated using the MODIS reflectance database as well as the TANSO-FTS. MODIS has wavelength bands similar to TANSO-CAI B2-4. Relations between simulation and observation radiances of B2-4 are obtained. The relations are estimated as almost linear and independent of time series.

4.1.2 Vicarious Calibration in the Ocean around Hawaii

This method evaluates B1, B2, and B4 relative to B3. Hence, B3 is desirable as a well-calibrated radiance. Aerosol optical depth is estimated from the B3 radiance. The other band radiances are calculated to agree with B3 aerosol information. B1 is contributed by Rayleigh scattering and normalized water leaving radiance (nLw). There was no appropriate database for nLw380nm in operation, while MOBY measured the nLw380nm in the ocean around Hawaii in 2003. The Aqua MODIS nLw412nm is observed simultaneous to the TANSO-CAI in operation. The relation of MOBY (nLw380nm) to MODIS (nLw412nm) in 2003 was used. Simulated radiance is calculated from the estimated nLw380nm and Rayleigh component. The relations between simulation and observation radiances of B1, B2, and B4 are obtained. The relations are estimated as almost linear and independent of time series.

4.1.3 Summary of the Radiometric Calibration

The TANSO-CAI calibration factor is described as the ratio of the referenced radiance relative to the Level 1B radiance, which is calculated using the radiometric conversion coefficient based upon the PFT result. The calibration factors of both methods are listed in Table 3. B2 results of the methods are different. B1 is different by more than 20 percent from the PFT results. One reason is that the dark count on orbit differs from the PFT results. The contribution is estimated at 3-5 percent. Initial calibration was restricted to the methods, sites, and data quantities; hence, further calibration will be required.

TANSO-CAI Calibration Factor (= Referenced radiance[*1] / Level 1B radiance)				
	B1	B2	B3	B4
Sahara Desert	N/A	0.992	1.019	1.079
Ocean around Hawaii[*2]	1.226	0.777	1	1.068

Table 3. TANSO-CAI radiometric calibration factor for bias correction (average from April to June).
(*1) Referenced radiance originated from Thuillier 2002. (*2) Relative calibration of B1, B2, and B4 to B3.

4.2 Geometric Calibration

Geometric accuracy of the TANSO-CAI is evaluated. B3 is the reference band of B1 and B2 for an array of 2000 pixels. The locations are evaluated using GCPs derived from the GSHHS. The absolute registrations of B3 and B4 are evaluated by Japanese coastlines observed on April 5, 8, 29, and May 2. Geometric errors in pixel and line directions of B3 and B4 are obtained. The systematic errors are estimated in a linear relation with pixel numbers in the cross-track direction. The systematic errors remained in the PFT geometric model. Absolute geometric accuracies of the TANSO-CAI are shown in Table 4. Relative registration accuracies of B1 and B2 to B3 are in Table 5. Geometric accuracies after correction are evaluated within the target accuracy of 0.9 km.

	B1	B2	B3	B4
Pixel (RMSE)	0.14 km	0.10 km	0.11 km	0.24 km
Line (RMSE)	0.10 km	0.13 km	0.13 km	0.33 km

Table 4. TANSO-CAI absolute geometric accuracy after bias correction.

	B1	B2
Pixel (σ)	0.09 pixel	0.01 pixel
Line (σ)	0.17 pixel	0.29 pixel

Table 5. TANSO-CAI relative registration accuracy after bias correction (B1 and B2 referenced to B3).

5. SUMMARY

The initial calibration and validation phase was completed on July 30. Intensive observation data was acquired for the initial calibration and validation. The calibration accuracies were evaluated on radiometry, geometry, and spectrometry. Geometric correction was applied to the TANSO-CAI Level 1 processing in view of the initial calibration result. The corrected geometric accuracy is within the target. The geometric accuracy of the TANSO-FTS was confirmed as within the target until May 2, while the following period has not yet been confirmed. The FTS radiometric accuracy is within the 10 percent target. The CAI is within the 10 percent target accuracy, except for B1. The radiometric evaluations are preliminary results because of the restricted conditions of area, period, and methods. Further evaluation will be required in the next period. We will confirm the calibration accuracies and improvement of Level 1 products for public release.

References

Kuze, A., H. Suto, M. Nakajima, and T. Hamazaki (2009), "Thermal and near infrared sensor for carbon observation Fourier-transform spectrometer on the Greenhouse Gases Observing Satellite for greenhouse gases monitoring," Appl. Opt. 48, 6716-6733.

Yokota T., H. Oguma, I. Morino, and G. Inoue, (2004), "A nadir looking SWIR FTS to monitor CO2 column density for Japanese GOSAT project," *Proc. 24th Int. Symp. Space Tech. Sci., Japan Society for Aeronautical and Space Sciences*, 887-889.

Yoshida, J., T. Kawashima, J. Ishida, K. Hamada, J. Tanii, Y. Katsuyama, H. Suto, A. Kuze, M. Nakajima, and T. Hamazaki, (2008), "Prelaunch performance test results of TANSO-FTS and CAI on GOSAT," *Proc. SPIE,* 7082, 708214.

Acknowledgements

We thank the members of the NIES, the GOSAT Science team, the CAI vicarious calibration team, Mitsubishi Space Software Co., Ltd., NEC, and NEC TOSHIBA Space Systems, Ltd. for their useful suggestions and cooperation.